Transcriptional Mechanisms of Thermal Acclimation in Prochlorococcus

Laura Alonso-Sáez, Antonio Palacio, Ana Cabello, Semidán Robaina-Estévez, José González, Laurence Garczarek, Ángel López-Urrutia

Transcriptional mechanisms of thermal acclimation in *Prochlorococcus*

Laura Alonso-Sáez, [a]# Antonio S. Palacio,[a] Ana M. Cabello,[a*] Semidán Robaina-Estévez,[b] Jose M. González,[b] Laurence Garczarek[c], Angel López-Urrutia[d]

[a]AZTI, Marine Research, Basque Research and Technology Alliance (BRTA), Sukarrieta, Spain

[b]Department of Microbiology, University of La Laguna, La Laguna, Spain

[c] Sorbonne Université, CNRS, UMR 7144 Adaptation and Diversity in the Marine Environment (AD2M), Station Biologique de Roscoff (SBR), Roscoff, France

[d] Centro Oceanográfico de Gijón (IEO), CSIC, Gijón, Asturias, Spain

#Address correspondence to Laura Alonso-Sáez, lalonso@azti.es

*Present address: Ana M. Cabello, Centro Oceanográfico de Málaga, Centro Nacional – Instituto Español de Oceanografía, Consejo Superior de Investigaciones Científicas (CSIC). Fuengirola, Málaga, Spain

Running head: Mechanisms of thermal acclimation in *Prochlorococcus*

Word count for abstract: 200 words

Word count for text: 5068 words

Abstract

Low temperature limits the growth and the distribution of the key oceanic primary producer *Prochlorococcus,* which does not proliferate above ca. 40 degrees latitude. Yet, the molecular basis of thermal acclimation in this cyanobacterium remains unexplored. We analyzed the transcriptional response of the strain *Prochlorococcus marinus* MIT9301 in long-term acclimations and in natural *Prochlorococcus* populations along a temperature range enabling its growth (17 to 30ºC). MIT9301 upregulated mechanisms of the global stress response at the temperature minimum (17ºC) but maintained the expression levels of genes involved in essential metabolic pathways (e.g., ATP synthesis, carbon fixation) along the whole thermal niche. Notably, their declining growth from the optimum to the minimum temperature was coincident with a transcriptional suppression of their photosynthetic apparatus and a dampening of its circadian expression patterns, indicating a loss in their regulatory capacity under cold conditions. Under warm conditions, the cellular transcript inventory of MIT9301 was strongly streamlined, which may also induce regulatory imbalances due to stochasticity in gene expression. The day-time transcriptional suppression of photosynthetic genes at low temperature was also observed in MIT9301-like populations across the global ocean, implying that this molecular mechanism may be associated with the restricted distribution of *Prochlorococcus* to temperate zones.

Importance

Prochlorococcus is a major marine primary producer with a global impact on atmospheric CO_2 fixation. This cyanobacterium is widely distributed across the temperate ocean, but virtually absent at latitudes above 40º for yet unknown reasons. Temperature has been suggested as a major limiting factor, but the exact mechanisms behind *Prochlorococcus* thermal growth restriction remain unexplored. This study brings us closer to understanding how *Prochlorococcus* functions under temperature challenging conditions, by focusing on its transcriptional response after long-term acclimation from its optimum to its thermal thresholds. Our results indicate a detrimental role of oxidative stress on *Prochlorococcus* fitness under cold conditions, as the drop in its growth rate was paralleled by a transcriptional suppression of the photosynthetic machinery during day-time, likely to mitigate the generation of ROS. Notably, warm temperature induced a marked shrinkage of its cellular transcript inventory, which may induce regulatory imbalances in the future functioning of this cyanobacterium.

Introduction

Prochlorococcus is the most abundant photosynthetic organism on Earth (1), and a major contributor to the oceanic primary production (2). Despite sustaining vast populations at the global scale, *Prochlorococcus* exhibits an enigmatic distribution in the ocean, with a sharp latitudinal barrier at ca. 45°N and 40°S (3, 4). While the ultimate reasons for such restricted distribution are still unknown and may involve biotic interactions (5), temperatures in the range of 12º-15ºC typically limit the growth of *Prochlorococcus* in culture (3, 6, 7) and *in situ* (3), potentially representing critical thresholds for their metabolism. Due to genome streamlining, *Prochlorococcus* is assumed to have a lower regulatory capacity than other phytoplankton groups, and a limited metabolic flexibility to adapt to environmental disturbance, including temperature changes (8–10). However, a mechanistic understanding of their temperature sensitivity at the molecular level is still lacking.

In general, addressing the impact of temperature on the functioning of any organism is complex, as this parameter has overriding effects on virtually every aspect of cell physiology. Temperature notably impacts the cellular size, the stability and conformation of macromolecules, and the kinetics of biochemical reactions, altogether leading to differences in cell growth (11). In the case of photosynthetic organisms such as *Prochlorococcus*, growth is closely linked to their photosynthetic capacity, which is also impacted by temperature (12–14). Under temperature conditions below the optimum, the slow-down in carbon fixation rates constrains the replenishment of final acceptors of the photosynthetic electron flow, producing an imbalance between photochemistry and metabolism. Under these conditions, the excess of light energy absorbed can generate cell-damaging reactive oxygen species (ROS), which need to be counterbalanced by photoprotective mechanisms (15). Under heat-stress conditions (35-50ºC) ROS are also

typically produced likely not as a result of an excess of energy absorbed, but of heat-induced structural and functional changes in the photosystems and thylakoid membranes (16). The decline in photosynthetic activity in phototrophs under moderate warm stress has been associated with different processes, including the inhibition of *de novo* synthesis of the photosystem II D1 protein by ROS (17), the inactivation of the oxygen-evolving complex (18) and declines in electron transport (19).

At the expression level, a variety of compensatory mechanisms have been found to be activated in several phytoplankton groups (i.e., *Synechococcus* and eukaryotic phytoplankton) to preserve cell functioning under thermal stress conditions (12–14, 20–23). The cold-stress response network involves the upregulation of fatty acid desaturases to offset decreases in membrane fluidity at low temperature, and RNA helicases and cellular chaperones to facilitate proper folding of nucleic acids and proteins (21, 22, 24, 25). Low temperature can also impact the expression of central components of the transcriptional and translational machinery in eukaryotic phytoplankton, which are upregulated to compensate for their reduced efficiency (21, 26), and even impact global regulatory networks such as circadian rhythms in cyanobacteria (27). At elevated temperatures, a nearly universal response induces the expression of heat-shock proteins, which degrade or restructure denatured proteins and nucleic acids (28).

Some of the temperature compensatory mechanisms involve only short-term transcriptional responses until cell functioning is restored (25). In other cases, the baseline expression of key enzymes is upregulated under long-term cold acclimations (26). Beyond short-term temperature manipulation experiments, where cells are suddenly exposed to a "thermal shock", understanding mechanisms of long-term acclimation is particularly relevant as they more accurately reflect responses to gradually changing thermal conditions. Here, we performed a series of experiments on *Prochlorococcus marinus* MIT9301,

where cells were progressively exposed from a temperature close to their optimum to their upper and lower thresholds of growth. This strain, which is a representative of the *Prochlorococcus* dominant clade *in situ* (HLII, (29, 30)), was selected because it shares the highest sequence similarity with environmental sequences (31) and enabled the identification of closely related transcripts in natural *Prochlorococcus* populations. We first used a quantitative RNA-Seq approach (32, 33) to decipher the transcriptional response of MIT9301 to temperature acclimations. Then, we addressed the environmental relevance of one of the most conspicuous transcriptional responses observed in MIT9301, involving highly expressed photosynthetic genes, in oceanic metatranscriptomes collected along a comparable thermal gradient. Our objective was to analyse how sustained growth at sub-optimal temperature reprograms the transcriptome of *Prochlorococcus* and significantly advance in our understanding of which mechanisms underlie their growth restriction under cold and warm conditions.

Results

Thermal acclimation experiments with *Prochlorococcus marinus* MIT9301: growth rates and mRNA content.

MIT9301 cultures were synchronized to a diel 12:12 light/dark cycle and long-term acclimated to six temperatures along their thermal range (Figure 1, Figure S1). MIT9301 could not survive single-generation transfers below 17ºC or above 30ºC degrees and, thus, these were considered thermal thresholds for this strain (T_{min} and T_{max}, hereinafter). The growth rate of MIT9301 increased from 0.17 day^{-1} at T_{min} to ca. 0.61 day^{-1} at 25ºC (hereinafter referred to as optimum growth temperature, T_{opt}) and, thereafter, entered a warm-stress zone up to 30ºC, where no further increases in growth rate were observed

(Figure 1A). The average size of MIT9301 cells also changed along the thermal gradient, with maximum and minimum values at the T_{min} and T_{max}, respectively (Figure 1A).

After the acclimation period, RNA samples were collected at different temperature conditions 3 hours after subjective sunrise and sunset (day- and night-time, respectively, hereinafter). Large variations in the number of mRNA transcripts per cell were found in replicate cultures acclimated to 17 and 20ºC during day-time, while values were highly constrained in temperatures close to the optimum (22 and 25ºC, Figure 1B). A pattern of decrease of mRNA transcripts with increasing temperature was found, with the average number of mRNA transcripts per cell being positively correlated with cellular size in night-time samples (Spearman *Rho* = 0.89, $p < 0.001$, Supplementary Figure S2).

Quantitative global transcriptomic analysis of MIT9301 in experimental long-term acclimations

Top-expressed genes in MIT9301 were associated with photosynthetic components (e.g., *psbA*, *psbC*), the RuBisCO enzyme (*rbcL*) or an ammonium transporter (*amt*), which reached average values above two mRNA transcripts per cell (Table S3). However, the average abundance of most mRNA transcripts was at least one order of magnitude below that value, which indicates that only a fraction of the population was actively expressing them at any given time. Estimates of mRNA transcript abundance were normalized by cell biovolume (i.e., transcripts per μm^3 or [mRNA], Table S4), to discard potential indirect effects of cell size on transcript abundance in further analyses.

A substantial fraction of MIT9301 genes were differentially expressed along the temperature gradient (i.e., exhibited significant variations in cellular [mRNA] estimates at different temperatures). In total, 61% of protein-coding MIT9301 genes were differentially expressed at night-time, while this number was reduced to 30% during day-

time (Kruskal-Wallis test, $p < 0.05$), in association with an increase in the variability of gene expression levels; while [mRNA] values of individual genes in different biological replicates were highly constrained at the T_{opt}, a large variation was found during day-time at both thresholds of growth, and particularly at the T_{min} (Figures 2 and 3, Table S4). This suggests a reduced ability of MIT9301 cells to maintain a tight transcriptional control under challenging temperature conditions when cells are exposed to light. Notably, the expression of some sigma factors and key regulatory proteins from different families also showed this pattern (Figures 3A and 3B).

We identified five clusters of genes according to their patterns of day and night-time expression at different temperatures (Figure 2, Table S5). More than 90% of MIT9301 protein-coding genes were assigned to one of these clusters with a probability score > 0.5), which indicates that these clusters were highly representative of the main thermal gene expression responses in this strain. Clusters A and E were represented by genes involved in core cellular and metabolic processes typically expressed in *Prochlorococcus* during day- and night-time, respectively (34). Clusters C and D were associated with mechanisms of cold-stress response, as they were characterized by a strong upregulation at the T_{min} either during day-time or both day- and nigh-time, respectively. Finally, the expression of genes in Cluster B showed a decreasing trend from the T_{opt} towards the T_{min} during day-time (Figure 2), paralleling the pattern observed in growth rates along the thermal niche (Figure 1A). Therefore, we hypothesize that the expression of Cluster B genes is associated with metabolic processes limiting the growth of *Prochlorococcus* when exposed to cold conditions.

Cluster A included genes related with C fixation and assimilation such as the RuBisCO (*rbcLS)*, CO_2 transporters *(csoS2*), carboxysome shell proteins (*ccmK*), the Calvin cycle (e.g., *gap2, tktA, glpX, pgk, cbbA*) and glycogen synthesis (*glgABC*), consistently

expressed during day-time along the thermal gradient (Figure 2, Tables S4-S5). This cluster also included ATP synthesis genes (*atpADE*) and a few components of the PS II (*psbA, psbC* and *psbD*). Cluster E included genes related to catabolic consumption (*cyoB, ndhD*), DNA replication (*dnaA, nrdJ, gyrB),* cell division (*ftsZYQ)* and the pentose phosphate pathway (*tal, gnd, zwf*), all of them upregulated at night-time. Altogether, these essential pathways likely represent a transcriptional core, which *Prochlorococcus marinus* MIT9301 maintains at all temperature conditions.

Clusters C and D genes included different elements of the global stress response (e.g., cellular chaperones such as *groES/groES, dnaK, clpBCP* (35, 36)), mechanisms of DNA repair (*recA, ruvB* (37, 38)), and the synthesis of antioxidant compounds such as carotenoids (*pds, crtBH)* and rubredoxin (*rub*) (Table S5). Notably, the expression of the chaperones *groEL/groES, grpE* and *htpG* were strongly upregulated at the T_{min} only during day-time, suggesting a prioritization of their expression during the light-exposed period (Figure 3C). Other metabolic processes upregulated at the T_{min} were the mobilization of energy storage (i.e., glycogen degradation, *glgP*), and the synthesis of proteins, as reflected by the increase in the [mRNA] of amino-acid synthesis genes (*glyA, serA, leuA*), translation initiation factors (*infABC*) and N acquisition genes (Figures 2 and 3, Table S4).

The strong upregulation of N acquisition mechanisms at the T*min* under light conditions was observed not only for genes predominately expressed during day-time at the T_{opt} (i.e., the global nitrogen regulatory protein *ntcA*, *glnA*, and urea transporters*)*, but also for genes typically expressed at night-time in *Prochlorococcus*, such as the ammonium transporter (*amt*) and urease genes (*ureABC*.) This likely reflects the large cellular demand of N for protein synthesis during day-time under cold stress conditions. In the case of phosphate uptake, the high affinity ABC transporter *pstABC* genes were upregulated under

cold conditions at night, following the pattern of cluster E genes, possibly related to the cellular demand of P for DNA replication. By contrast, both copies of the periplasmic phosphate binding protein (*pstS*) showed maximum expression values around the T_{opt} during day-time following the pattern of most photosynthetic genes (cluster B), which highlights the complexity in the thermal response of nutrient acquisition genes (Figure 3D).

Finally, the expression of all components of the PS I complex (*psaABDEFKL*) and some of the PS II (including *psbBJH* and the oxygen evolving complex protein *psb*O) showed a gradual decrease in expression from a temperature close to the optimum to the $T_{min,}$ (Figure 2) in correlation with MIT9301 growth rates (Figure 1). This expression pattern was different from other PSII components (*psbACD*, see above), which were not differentially expressed during day-time along the thermal niche (Kruskall-Wallis, $p > 0.05$, Figure 2). Similarly, many components of the photosynthetic electron transport genes were assigned to either Cluster B (*petACGNM*) or Cluster A (*petBEDH)*, implying a non-uniform transcriptional thermal response of all components of the photosynthetic apparatus (Figure 4). Yet, a general pattern of upregulation of photosynthetic genes during night-time under cold conditions, inducing changes in their day-night log2fold expression ratio was observed (Figure 2), suggesting a loss in the capacity of the cells to regulate their circadian expression.

Transcriptional response of photosynthetic genes in naturally occurring *Prochlorococcus* populations

With the aim of testing whether the transcriptional suppression of photosynthetic genes at cold temperature observed in MIT931 was also found in natural *Prochlorococcus* populations *in situ*, we identified reads closely related to MIT9301 in the *Tara* Oceans metatranscriptome dataset (39) including samples distributed across different ocean

basins along a comparable thermal gradient (Table S6). The number of MIT9301-like reads ranged from 6379 to 9.62 million in the different environmental samples (Table S7). The DESeq2 normalized abundance of transcript counts from some of the most actively expressed genes of the PSII (*psbA*, *psbD*) did not show any significant trend along the *in situ* thermal gradient from 17 to 30ºC (Spearman correlation, $p > 0.05$), mirroring the response observed under culture conditions (Figure 5, Supplementary Figure S3). By contrast, other PSII components (*psbJ*) were positively correlated with temperature both in the experimental and *in situ* datasets (Spearman $R = 0.6$, $p < 0.01$), indicating a downregulation at cold temperature (Figure 5). Similarly, the downregulation of PS I genes at cold temperature was clearly observed both in the experimental and *in situ* dataset (Figure 5), reinforcing the environmental relevance of this response. Temperature had the strongest correlation to photosynthetic transcript counts in comparison with all other tested environmental variables (Supplementary Figure S4), excluding the possibility that these correlations were driven by co-varying environmental parameters.

Discussion

There is a remarkable gap of fundamental knowledge on the molecular mechanisms of thermal acclimation in *Prochlorococcus*, as previous studies have concentrated on their cyanobacterial sister clade *Synechococcus* and eukaryotic phytoplankton (12–14, 20–22, 40, 41). Acquiring this knowledge would be crucial towards answering a long-standing question: what limits the ability of *Prochlorococcus* to expand to high-latitude environments? The decrease in the light-harvesting capacity of phytoplankton under cold conditions has been typically attributed to changes in the conformation of membrane lipids and proteins of their photosynthetic apparatus (14, 42). Our quantitative gene expression

analysis shows that, in the case of *Prochlorococcus*, the inability to maintain their photosynthetic capacity under cold conditions is already critically compromised at the transcriptional level, as we found a clear suppression of the expression of most photosynthetic genes towards cold conditions. The same pattern was found for MIT9301-like reads in *in situ* metatranscriptomes across the global ocean, suggesting that this molecular mechanism may be relevant to explain the restricted distribution of *Prochlorococcus* to temperate zones. Notably, this response differs from previous studies targeting diatom cultures (26), or phytoplankton communities *in situ* (21, 39) , indicating fundamental differences in the ability of *Prochlorococcus* to respond to cold temperature, which may be related to their exceptional high sensitivity to oxidative stress (38, 43).

Photosystems are naturally sensitive to light damage, which is exacerbated under low temperature (22). The cellular decision of shutting down their sunlight energy conversion system at cold conditions likely arises from the inability of *Prochlorococcus* to cope with uncontrolled redox chemistry when there is an imbalance between the production of excited electrons by light and their metabolic consumption. The downregulation of photosystems would represent an emergency mechanism to slow-down the electron flow and prevent the production of cell-damaging ROS. Notably, the response was not equal for all photosystem components, as previously observed in cultured *Prochlorococcus* strains undergoing other types of stress, such as iron starvation (44), phage infection (45), or high-light exposure (46). On the one hand, the high expression of *psbA* transcripts at all temperature conditions is likely related to the need to maintain an exceptionally high turnover rate of this protein (47), being differentially regulated than other PS components (34, 48, 49). On the other hand, the selective downregulation of PSI probably arises from the strong need to protect PSI from oxidative stress, as this photosystem typically lacks efficient repair machinery, and therefore its damage may be practically irreversible (50).

Interestingly, MIT9301 also upregulated the plastoquinol terminal oxidase (PTOX) at the T_{min} (Figure 2), which is thought to function as a safety valve in cyanobacteria to avoid electron flow towards PSI (51).

In addition to the transcriptional suppression of photosynthetic genes, we found that under light conditions, cold temperature induced a loss in the regulatory capacity of MIT9301 cells. This was reflected in the loss of the circadian day/night gene expression ratio and the increased variability in the concentration of cellular mRNA transcripts among biological replicates. In a previous study, it has been suggested that higher levels of stochasticity in *Prochlorococcus*' gene expression during the transition from photosynthesis to the use of internal energy is related to the accumulation of ROS (52). Our transcriptomic results are consistent with the idea of oxidative stress impacting the regulatory capacity of *Prochlorococcus*. Notably, at the T_{min} we observed a high variability in the expression of regulatory proteins that modulate the cellular response to daily light fluctuations in cyanobacteria, including sigma factors (*rpoD*) (53, 54), the NblS-RpaB two-component system (55) and the SasA-RpaA clock output system(56, 57). Assuming that mRNA transcript levels reflect the protein levels of these regulators, our results would imply a critical impairment of their co-regulated networks. Other mechanisms of transcriptional regulation in *Prochlorococcus* (i.e., RNA-based regulatory strategies (58)), were likely also compromised at low temperature, as evidenced by the upregulation of the ribonuclease *rne* gene at the T_{min} (Table S4).

Marked changes in the day/night gene expression ratio of some of *Prochlorococcus* key functional genes along the thermal niche imply a deregulation of one of their fundamental features, i.e., the coordination of transcriptional oscillations with the daily light/dark cycle. This feature is key to optimize cellular processes through anticipating and synchronizing transcription of photosynthetic genes with daylight hours (34, 59, 60). At T_{opt}, the

day/night expression *preferenda* of most key functional genes of MIT9301 matched those previously observed in the model strain MED4 (34), reinforcing the idea that maintaining this transcriptional choreography is a highly conserved and critical trait. The deregulation observed at cold temperature led to the paradoxical situation where, after subjective sunrise, chilled *Prochlorococcus* MIT9301 cells contained several-fold less PSI transcripts than after subjective sunset, which supports the idea of a malfunctioning regulatory network. With only two samplings over the daily cycle, we cannot ensure whether the observed changes were due to random misregulations or variations in the phasing or amplitude of their diel gene expression patterns. Yet, considering that we were sampling the two daily periods when most *Prochlorococcus* genes show maxima in expression (34), the inversion of their day/night *preferenda* is remarkable and likely has an important impact on its fitness.

By contrast to the pattern observed in day-time samples, genes related to *Prochlorococcus* cell division cycle, typically expressed during night-time, showed rather constrained [mRNA] values between replicates. We observed an increase in [mRNA] of those genes towards cold conditions, which may be related to the predominant cell cycle phase of the cells. As the timing of cell division is delayed in *Prochlorococcus marinus* MIT9301 when acclimated to cold temperature (61), our results likely reflect a situation where a higher proportion of cells were still undergoing the S phase at 17ºC and 20ºC at the time of sampling (i.e., 3 hours after subjective dusk), as compared to other acclimation temperatures.

At the warm temperature threshold, the upregulation of a variety of cellular chaperones (e.g., *groEL/groES, htpG, grpE*) reflected that cells were undergoing substantial stress. However, no drastic changes were generally observed in the expression of most protein-coding genes at the T_{max}. Accordingly, a previous study on the short-term response of

MED4 to warm stress found that the synthesis of new polypeptides was not induced (62). We had previously shown that *Prochlorococcus* MIT9301 cells decrease in size after long-term warm acclimation, in accordance with the temperature-size rule (61). Interestingly, here, our quantitative transcriptomic approach showed a conspicuous streamlining in the transcript inventory in the cells in parallel with the progressive reduction in cell size. While at non-restricting growth temperature the average estimate of mRNA transcript abundance per cell was within the range reported for environmental marine bacteria (i.e., ca. 85-255 transcripts per cell (32)), under warm conditions this average dropped down to 30 mRNA transcripts of protein-coding genes per cell at night-time. Cellular reactions involving small numbers of molecules are intrinsically noisy, being dominated by fluctuations in concentration and stochasticity (63, 64). Thus, the decline in the transcript inventory under warm conditions invites the hypothesis that there is a critical threshold in the number of mRNA copies beyond which cells lose regulatory capacity, contributing to the growth arrest.

In summary, previous studies on phytoplankton have identified the cellular membrane and translational apparatus as central elements associated with the thermal adaptation at the transcriptional level (21, 26). Some of these mechanisms were also observed in MIT9301, such as the upregulation of the translational machinery, likely to compensate the general slow-down in protein synthesis rates under cold conditions (24). Yet, we found that in the case of *Prochlorococcus*, oxidative stress emerged as a major factor impacting its physiology when approaching cold temperature, as this source of stress relates to both the need to protect the photosynthetic machinery and the ability of *Prochlorococcus* to "reset" their daily cycles in the morning hours (65). Cold temperature has been previously shown to nullify the circadian rhythm in different organisms, including plants and different phytoplankton species, moving the circadian oscillation to a

damped oscillation (see references in (27)). As *Prochlorococcus* contains only a minimalist circadian system, their cell cycle is likely more easily perturbated than that from organisms containing a complete *kaiABC* gene set.

The disruption of the transcriptional choreography in *Prochlorococcus* may be a differentiating factor as compared to *Synechococcus* and eukaryotic phytoplankton, which do not require maintaining such a finely tuned daily expression rhythm to maintain their metabolism. The higher tolerance of *Synechococcus* to oxidative stress(38) may also imply a more resilient photochemistry when exposed to cold conditions, enabling them to colonize higher latitudes. Additionally, we postulate that increased levels of stochasticity in gene expression at temperature challenging conditions may contribute to a decrease in *Prochlorococcus* fitness. These remains as an interesting hypotheses to test in future studies, with implications for the functioning of this global primary producer and, thus, the marine carbon biogeochemistry in future oceanic conditions.

Materials and Methods

Growth of cultures and temperature acclimation

We grew non-axenic cultures of *Prochlorococcus marinus* MIT9301 obtained from the Roscoff Culture Collection (RCC) in PCR-S11 culture medium (66) based on Red Sea Salt (Houston, TX, USA). Cultures were grown under a 12:12 hour photoperiod and irradiance of 120 µmol quanta $m^{-2}s^{-1}$ in polycarbonate flasks with vented caps. During the acclimation, we maintained the cultures in exponential growth by performing serial transfers before cell density reached 30% of the maximum yield. The acclimation started from 22ºC (i.e., temperature of maintenance in RCC) and temperature was progressively changed towards the upper and lower thermal thresholds. At each acclimation step,

temperature was changed by a maximum of 2ºC and down to 0.2ºC when approaching the temperature thresholds, to avoid lethal thermal stress (Figure S1). We considered that the culture had been fully acclimated to a temperature treatment when growth rate stayed stable in at least two consecutive growth curves after at least 8 generations. Flow cytometry was used for sustained monitoring of the culture growth during the acclimation process. Samples were fixed with glutaraldehyde (final concentration of 0.025%) for 10 minutes at room temperature and dark conditions, and frozen at -80°C until analysis in a FACSCalibur flow cytometer (Becton Dickinson). Estimates of cell size were obtained based on the natural logarithmic-transformed side scatter (SSC) using the calibration provided in (67) and assuming a spherical cellular shape.

RNA samples collection and extraction

Once the cultures reached full acclimation to the temperatures selected (17, 20, 22, 25 and 30°C), we re-inoculated biological replicate batch cultures into fresh medium (160 mL) and collected samples for RNA-Seq analysis during exponential growth (with cell density values ranging between 6 to 17 10^7 cells mL^{-1}, Table S1). For each temperature and biological replicate (ranging from 3 to 7, depending on the experimental treatment, Table S1), samples for RNA extraction were collected 3 hours after the onset and offset of the photoperiod (day- and night-time, respectively). Exceptionally, for the acclimation temperature 22ºC, only day-time RNA samples were available. Samples were filtered on 0.22-µm pore-size PES filters using a vacuum pump at a pressure of 5 psi. Immediately after filtration, filters were snap frozen in liquid nitrogen and stored at -80°C. The time elapsed from the start of the filtration until freezing was always lower than 2 minutes.

Quantitative benchmarked RNA extraction was performed following (33) using five RNA standards from *Saccharolobus* (*Sulfolobus*) *solfataricus* P2 (NCBI Taxon ID 273057) obtained by *in vitro* transcription of genomic templates of the isolate (standards 3, 6, 7,

13 and 14, as described in (33)). The RNA standards were individually spiked (10 to 28 µL) at a concentration of ca. 20 pg μL^{-1} to the filters prior to the initiation of the RNA extraction. Subsequently, RNA samples were extracted with the mirVana kit (Ambion), and DNA was removed using the TURBO DNase (Ambion). Samples were depleted from ribosomal RNA using the Ribo-Zero rRNA removal kit (Bacteria, Illumina) and quality check was performed using a Bioanalyzer (Agilent). mRNA samples were concentrated using the Zimo Clean & Concentrator kit, and cDNA libraries were constructed using the TruSeq Stranded mRNA Sample Preparation Kit (Illumina). cDNA libraries were sequenced as 75bp paired-end reads on an Illumina HiSeq v4 platform (CNAG, Spain). Raw reads have been submitted to ENA under project accession number PRJEB54738.

Quantitative gene expression analysis of *Prochlorococcus* MIT9301 under culturing conditions

Sequence read quality check was performed with the FastQC tool (68), and Trimmomatic (69) was used to trim raw sequences (SLIDINGWINDOW:50:35 and MINLEN:50) and pair those passing quality thresholds. rRNA sequences were removed using SortMeRNA (70) and the remaining reads were mapped with Bowtie2 (71) (using the '–non-deterministic' parameter) against the *Prochlorococcus marinus* MIT9301 genome (NCBI Taxon ID 167546). The same procedure was done with the *S. solfataricus* genome to identify RNA internal standard reads. Read count tables were obtained using HTSeq (72) with the following parameters: '–stranded = reverse -a 10 -m intersection-nonempty'. Quantitative estimates of individual transcript abundance (Ta) of MIT9301 protein-coding genes in each RNA sample were obtained following the calculations described in (73):

$$Ta = (Ts \times Sa)/Ss$$

where Ta corresponds to the estimated number of transcripts of an individual MIT9301 protein-coding gene, Ts corresponds to the number of reads assigned to the corresponding

MIT9301 protein-coding gene, Sa corresponds to the molecules of internal RNA standards spiked to the RNA sample, and Ss corresponds to the number of reads assigned to *S. solfataricus* internal standards. In this calculation, one of the standards (standard 14) was removed from the analysis because it was consistently recovered in higher proportion than other standards. Ta values were divided by total cell abundance or estimates of total cell biovolume collected in the corresponding RNA filter to obtain estimates of transcript abundance per cell and per volume (i.e., transcript concentration), respectively (Tables S1- S3). This normalization is relevant because cell size, which varies over the thermal gradient in this strain (see Figure 1A), can impact the number of cellular transcripts (74, 75).

Bioinformatic analysis of transcriptional patterns of *Prochlorococcus* photosynthetic genes in oceanic samples and culture conditions

For comparing the expression patterns of *Prochlorococcus* photosynthetic genes along the same thermal gradient under environmental and culturing conditions, two datasets were produced using a common normalization method (DESeq2 (76)). The experimental dataset was obtained from the raw read counts obtained by HTSeq2 in the long-term thermal acclimation experiments, as explained above. For obtaining the environmental database, a dataset of *Tara* Oceans metatranscriptomes (39) was initially selected based on the latitude range where *Prochlorococcus* is found in the ocean (i.e., between 45º N and S), the thermal range of MIT9301 (17ºC to 30ºC), and the time of sample collection (between 6 and 12 am, when the expression of photosynthetic genes should be close to their maximum). Fastq sequence files were quality filtered with fastp (77) using default parameters, and rRNA sequences were removed with RiboDetector (78) with the option "--ensure" selected. The remaining reads were filtered to remove reads not affiliated with *Prochlorococcus*, using a custom made database with the complete genome sequences in

the MarRef database, which included 16 *Prochlorococcus* genomes (79), and eukaryotic genes of interest extracted from Refseq (80) (i.e., *psaA*, *psaB*, *psaD*, *psaF*, *psaL*, *psbA*, *psbD*, and *psbO*, searched with Entrez filter [Gene Name] AND ((protists[filter] OR plants[filter]) AND refseq[filter]). Metatranscriptome sequences closest to *Prochlorococcus* were identified based on Blastn v.2.12.0+ searches (identity ≥ 98% and bitscore ≥ 30), and only those with highest bitscore to *Prochlorococcus* sequences were considered further. Subsequently, we applied a two-step filtering strategy to obtain read counts closely related to MIT9301. First, we aligned each metatranscriptome sample against MIT9301 genome using BWA mem version 0.7.17-r1188 with default parameters (81). Next, we discarded alignments which had a percent identity lower than 98%, a read length lower than 50 bases, and a number of matches lower than 50% of the total length of each aligned sequence. Percent identity was computed as 100 × (N_m / (N_m + N_i)), where N_m corresponds to the number of matches in the alignment and N_i to the number of mismatches. The number of matches was obtained by parsing the MD tag of the alignment record, while the number of matches and mismatches was obtained from the CIGAR string in the SAM file. Once alignments were filtered, we proceeded to count aligned reads with HTSeq v.2.0. with default parameters (82). Next, we removed non-coding genes from the count matrices as well as genes which had no counts across all conditions, to facilitate the consequent normalization. We also discarded samples which had counts in less than 10 genes other than the *psbA* gene. Finally, we normalized count data using the default DESeq2 v.3.15 count normalization workflow (76). All analyses were assisted with customized Python code (83) available at https://github.com/Robaina/prochlorococcus.

Softclustering and statistical analyses

Clusters of differentially expressed genes that responded similarly over the thermal gradient were identified using softclustering, following (84). A matrix of N genes x 9 treatments (4 temperatures at night-time and 5 temperatures at day-time) was used as input data. Data for each gene was standardized to zero mean and unit variance. The optimal value of the parameter m in the Mfuzz algorithm was estimated through randomization following (85). The number of clusters was chosen to maximize the functional enrichment of gene clusters (COGs) and the ClusterJudge method (86). The standardized data was clustered by a generalized version of the fuzzy c-means algorithm. Finally, statistically significant differences in cellular transcript concentration among temperature regimes were determined by the Kruskall-Wallis test using R.

Acknowledgements: We are grateful to the Spanish Ministry of Economy and Competitiveness (MINECO) for supporting LA-S's Ramón y Cajal research contract (RYC-2012-11404), AP's FPI Ph.D. fellowship (BES2015076149) and the project TECCAM (CTM2014-58564-R) and the Spanish Ministry of Science and Innovation for supporting the project CYADES (RTI2018-100690-B-I00). SRE and JMG were supported by project PID2019-110011RB-C32 (Spanish Ministry of Science and Innovation, Spanish State Research Agency, doi: 10.13039/501100011033). L.G acknowledges funding from the Agence Nationale de la Recherche project CINNAMON (ANR-17-CE2-0014-01). This paper is contribution number (to be updated) from AZTI (Marine Research Division).

References

1. Partensky F, Hess WR, Vaulot AD. 1999. *Prochlorococcus*, a Marine Photosynthetic Prokaryote of Global Significance. Microbiology and Molecular Biology Reviews 63: 106-127

2. Li W. 1994. Primary production of prochlorophytes, cyanobacteria, and eucaryotic ultraphytoplankton: Measurements from flow cytometric sorting. Limnol Oceanogr 39:169–175.

3. Johnson ZI, Zinser ER, Coe A, McNulty NP, Woodward EMS, Chisholm SW. 2006. Niche partitioning among *Prochlorococcus* ecotypes along ocean-scale environmental gradients. Science (80-) 311:1737–1740.

4. Flombaum P, Gallegos JL, Gordillo RA, Rincón J, Zabala LL, Jiao N, Karl DM, Li WKW, Lomas MW, Veneziano D, Vera CS, Vrugt JA, Martiny AC. 2013. Present and future global distributions of the marine Cyanobacteria *Prochlorococcus* and *Synechococcus*. Proc Natl Acad Sci U S A 110:9824–9829.

5. Follett CL, Dutkiewicz S, Ribalet F, Zakem E, Caron D, Armbrust EV, Follows MJ. 2022. Trophic interactions with heterotrophic bacteria limit the range of *Prochlorococcus*. Proc Natl Acad Sci U S A 119:1–10.

6. Zinser ER, Johnson ZI, Coe A, Karaca E, Veneziano D, Chisholm SW. 2007. Influence of light and temperature on *Prochlorococcus* ecotype distributions in the Atlantic Ocean. Limnol Oceanogr 52:2205–2220.

7. Moore LR, Goericke R, Chisholm SW. 1995. Comparative physiology of *Synechococcus* and *Prochlorococcus*: Influence of light and temperature on growth, pigments, fluorescence and absorptive properties. Mar Ecol Prog Ser

116:259–276.

8. Scanlan DJ, Ostrowski M, Mazard S, Dufresne A, Garczarek L, Hess WR, Post AF, Hagemann M, Paulsen I, Partensky F. 2009. Ecological Genomics of Marine Picocyanobacteria. Microbiol Mol Biol Rev 73:249–299.

9. Partensky F, Garczarek L. 2010. *Prochlorococcus*: Advantages and limits of minimalism. Ann Rev Mar Sci 2:305–331.

10. Mary I, Vaulot D. 2003. Two-component systems in *Prochlorococcus* MED4: Genomic analysis and differential expression under stress. FEMS Microbiol Lett 226:135–144.

11. Kingsolver JG. 2009. The well-temperatured biologist. Am Nat 174:755–768.

12. Mackey KRM, Paytan A, Caldeira K, Grossman AR, Moran D, Mcilvin M, Saito MA. 2013. Effect of temperature on photosynthesis and growth in marine *Synechococcus* spp. Plant Physiol 163:815–829.

13. Pittera J, Humily F, Thorel M, Grulois D, Garczarek L, Six C. 2014. Connecting thermal physiology and latitudinal niche partitioning in marine *Synechococcus*. ISME J 8:1221–1236.

14. Pittera J, Partensky F, Six C. 2017. Adaptive thermostability of light-harvesting complexes in marine picocyanobacteria. ISME J 11:112–124.

15. Bailey S, Grossman A. 2008. Photoprotection in Cyanobacteria: Regulation of Light Harvesting. Photochem Photobiol 84:1410–1420.

16. Yamamoto Y. 2016. Quality control of photosystem II: The mechanisms for avoidance and tolerance of light and heat stresses are closely linked to membrane fluidity of the thylakoids. Front Plant Sci. Frontiers Media S.A.

https://doi.org/10.3389/fpls.2016.01136.

17. Murata N, Takahashi S, Nishiyama Y, Allakhverdiev SI. 2007. Photoinhibition of photosystem II under environmental stress. Biochim Biophys Acta - Bioenerg 1767:414–421.

18. Pospíšil P, Tyystjärvi E. 1999. Molecular mechanism of high-temperature-induced inhibition of acceptor side of Photosystem II. Photosynth Res 62:55–66.

19. Mathur S, Agrawal D, Jajoo A. 2014. Photosynthesis: Response to high temperature stress. J Photochem Photobiol B Biol 137:116–126.

20. Varkey D, Mazard S, Ostrowski M, Tetu SG, Haynes P, Paulsen IT. 2016. Effects of low temperature on tropical and temperate isolates of marine Synechococcus. ISME J 10:1252–1263.

21. Toseland A, Daines SJ, Clark JR, Kirkham A, Strauss J, Uhlig C, Lenton TM, Valentin K, Pearson GA, Moulton V, Mock T. 2013. The impact of temperature on marine phytoplankton resource allocation and metabolism. Nat Clim Chang 3:979–984.

22. Guyet U, Nguyen NA, Doré H, Haguait J, Pittera J, Conan M, Ratin M, Corre E, Le Corguillé G, Brillet-Guéguen L, Hoebeke M, Six C, Steglich C, Siegel A, Eveillard D, Partensky F, Garczarek L. 2020. Synergic Effects of Temperature and Irradiance on the Physiology of the Marine *Synechococcus* Strain WH7803. Front Microbiol 11:1–22.

23. Roth Rosenberg D, Haber M, Goldford J, Lalzar M, Aharonovich D, Al-Ashhab A, Lehahn Y, Segrè D, Steindler L, Sher D. 2021. Particle-associated and free-living bacterial communities in an oligotrophic sea are affected by different

592 environmental factors. Environ Microbiol 23:4295–4308.

593 24. Mikami K, Murata N. 2003. Membrane fluidity and the perception of
594 environmental signals in cyanobacteria and plants. Prog Lipid Res. Elsevier Ltd
595 https://doi.org/10.1016/S0163-7827(03)00036-5.

596 25. Los DA, Murata N. 1999. Responses to cold shock in cyanobacteria. J Mol
597 Microbiol Biotechnol 1:221–230.

598 26. Liang Y, Koester JA, Liefer JD, Irwin AJ, Finkel Z V. 2019. Molecular
599 mechanisms of temperature acclimation and adaptation in marine diatoms. ISME
600 J 13:2415–2425.

601 27. Murayama Y, Kori H, Oshima C, Kondo T, Iwasaki H, Ito H. 2017. Low
602 temperature nullifies the circadian clock in cyanobacteria through Hopf
603 bifurcation. Proc Natl Acad Sci U S A 114:5641–5646.

604 28. Rajaram H, Chaurasia AK, Apte SK. 2014. Cyanobacterial heat-shock response:
605 Role and regulation of molecular chaperones. Microbiol (United Kingdom)
606 160:647–658.

607 29. Farrant GK, Doré H, Cornejo-Castillo FM, Partensky F, Ratin M, Ostrowski M,
608 Pitt FD, Wincker P, Scanlan DJ, Iudicone D, Acinas SG, Garczarek L. 2016.
609 Delineating ecologically significant taxonomic units from global patterns of
610 marine picocyanobacteria. Proc Natl Acad Sci U S A 113:E3365–E3374.

611 30. Huang S, Wilhelm SW, Harvey HR, Taylor K, Jiao N, Chen F. 2012. Novel
612 lineages of *Prochlorococcus* and *Synechococcus* in the global oceans. ISME J
613 6:285–297.

614 31. Kettler GC, Martiny AC, Huang K, Zucker J, Coleman ML, Rodrigue S, Chen F,

615 Lapidus A, Ferriera S, Johnson J, Steglich C, Church GM, Richardson P,
616 Chisholm SW. 2007. Patterns and implications of gene gain and loss in the
617 evolution of *Prochlorococcus*. PLoS Genet 3:2515–2528.

618 32. Moran MA, Satinsky B, Gifford SM, Luo H, Rivers A, Chan LK, Meng J,
619 Durham BP, Shen C, Varaljay VA, Smith CB, Yager PL, Hopkinson BM. 2013.
620 Sizing up metatranscriptomics. ISME J https://doi.org/10.1038/ismej.2012.94.

621 33. Gifford SM, Becker JW, Sosa OA, Repeta DJ, DeLong EF. 2016. Quantitative
622 transcriptomics reveals the growth- and nutrient- dependent response of a
623 streamlined marine methylotroph to methanol and naturally occurring dissolved
624 organic matter. MBio 7.

625 34. Zinser ER, Lindell D, Johnson ZI, Futschik ME, Steglich C, Coleman ML,
626 Wright MA, Rector T, Steen R, McNulty N, Thompson LR, Chisholm SW. 2009.
627 Choreography of the transcriptome, photophysiology, and cell cycle of a minimal
628 photoautotroph, *Prochlorococcus*. PLoS One 4.

629 35. Bae W, Xia B, Inouye M, Severinov K. 2000. *Escherichia coli* CspA-family
630 RNA chaperones are transcription antiterminators. Proc Natl Acad Sci U S A
631 97:7784–7789.

632 36. Watanabe S, Sato M, Nimura-Matsune K, Chibazakura T, Yoshikawa H. 2007.
633 Protection of psbAII transcript from ribonuclease degradation in vitro by DnaK2
634 and DnaJ2 chaperones of the cyanobacterium *Synechococcus elongatus* PCC
635 7942. Biosci Biotechnol Biochem 71:279–282.

636 37. Bagby SC, Chisholm SW. 2015. Response of *Prochlorococcus* to varying CO
637 2 :O 2 ratios. ISME J 9:2232–2245.

638 38. Mella-Flores D, Six C, Ratin M, Partensky F, Boutte C, Le Corguillé G, Marie D,
639 Blot N, Gourvil P, Kolowrat C, Garczarek L. 2012. *Prochlorococcus* and
640 *Synechococcus* have evolved different adaptive mechanisms to cope with light
641 and uv stress. Front Microbiol 3:285.

642 39. Salazar G, Paoli L, Alberti A, Huerta-Cepas J, Ruscheweyh HJ, Cuenca M, Field
643 CM, Coelho LP, Cruaud C, Engelen S, Gregory AC, Labadie K, Marec C,
644 Pelletier E, Royo-Llonch M, Roux S, Sánchez P, Uehara H, Zayed AA, Zeller G,
645 Carmichael M, Dimier C, Ferland J, Kandels S, Picheral M, Pisarev S, Poulain J,
646 Acinas SG, Babin M, Bork P, Boss E, Bowler C, Cochrane G, de Vargas C,
647 Follows M, Gorsky G, Grimsley N, Guidi L, Hingamp P, Iudicone D, Jaillon O,
648 Kandels-Lewis S, Karp-Boss L, Karsenti E, Not F, Ogata H, Pesant S, Poulton N,
649 Raes J, Sardet C, Speich S, Stemmann L, Sullivan MB, Sunagawa S, Wincker P.
650 2019. Gene Expression Changes and Community Turnover Differentially Shape
651 the Global Ocean Metatranscriptome. Cell 179:1068-1083.e21.

652 40. Six C, Ratin M, Marie D, Corre E. 2021. Marine *Synechococcus*
653 picocyanobacteria: Light utilization across latitudes. Proc Natl Acad Sci U S A
654 118:1–11.

655 41. Ferrieux M, Dufour L, Doré H, Ratin M, Guéneuguès A, Chasselin L, Marie D,
656 Rigaut-Jalabert F, Le Gall F, Sciandra T, Monier G, Hoebeke M, Corre E, Xia X,
657 Liu H, Scanlan DJ, Partensky F, Garczarek L. 2022. Comparative
658 Thermophysiology of Marine *Synechococcus* CRD1 Strains Isolated From
659 Different Thermal Niches in Iron-Depleted Areas. Front Microbiol 13.

660 42. Pittera J, Jouhet J, Breton S, Garczarek L, Partensky F, Maréchal É, Nguyen NA,
661 Doré H, Ratin M, Pitt FD, Scanlan DJ, Six C. 2018. Thermoacclimation and

genome adaptation of the membrane lipidome in marine *Synechococcus*. Environ Microbiol 20:612–631.

43. Ma L, Calfee BC, Morris JJ, Johnson ZI, Zinser ER. 2018. Degradation of hydrogen peroxide at the ocean's surface: The influence of the microbial community on the realized thermal niche of *Prochlorococcus*. ISME J 12:473–484.

44. Thompson, Huang K, Saito MA, Chisholm SW. 2011. Transcriptome response of high- and low-light-adapted *Prochlorococcus* strains to changing iron availability. ISME J 5:1580–1594.

45. Thompson LR, Zeng Q, Chisholm SW. 2016. Gene expression patterns during light and dark infection of *Prochlorococcus* by cyanophage. PLoS One 11:1–20.

46. Steglich C, Futschik M, Rector T, Steen R, Chisholm SW. 2006. Genome-wide analysis of light sensing in *Prochlorococcus*. J Bacteriol 188:7796–7806.

47. Mattoo AK, Giardi MT, Raskind A, Edelman M. 1999. Dynamic metabolism of photosystem II reaction center proteins and pigments. Physiol Plant 107:454–461.

48. Garczarek L, Partensky F, Irlbacher H, Holtzendorff J, Babin M, Mary I, Thomas JC, Hess WR. 2001. Differential expression of antenna and core genes in *Prochlorococcus* PCC 9511 (Oxyphotobacteria) grown under a modulated light-dark cycle. Environ Microbiol 3:168–175.

49. Holtzendorff J, Partensky F, Mella D, Lennon JF, Hess WR, Garczarek L. 2008. Genome streamlining results in loss of robustness of the circadian clock in the marine cyanobacterium *Prochlorococcus marinus* PCC 9511. J Biol Rhythms

685 23:187–199.

686 50. Sonoike K. 2011. Photoinhibition of photosystem I. Physiol Plant 142:56–64.

687 51. Bailey S, Melis A, Mackey KRM, Cardol P, Finazzi G, van Dijken G, Berg GM,
688 Arrigo K, Shrager J, Grossman A. 2008. Alternative photosynthetic electron flow
689 to oxygen in marine *Synechococcus*. Biochim Biophys Acta - Bioenerg
690 1777:269–276.

691 52. Biller SJ, Coe A, Roggensack SE, Chisholm W. 2018. Heterotroph Interactions
692 Alter *Prochlorococcus* Transcriptome. mSystems 3:1–18.

693 53. Imamura S, Asayama M. 2009. Sigma Factors for Cyanobacterial Transcription.
694 Gene Regul Syst Bio 3:GRSB.S2090.

695 54. Summerfield TC, Sherman LA. 2007. Role of sigma factors in controlling global
696 gene expression in light/dark transitions in the cyanobacterium *Synechocystis sp*.
697 strain PCC 6803. J Bacteriol 189:7829–7840.

698 55. Van Waasbergen LG, Dolganov N, Grossman AR. 2002. nblS, a gene involved in
699 controlling photosynthesis-related gene expression during high light and nutrient
700 stress in *Synechococcus elongatus* pcc 7942. J Bacteriol 184:2481–2490.

701 56. Espinosa J, Boyd JS, Cantos R, Salinas P, Golden SS, Contreras A. 2015. Cross-
702 talk and regulatory interactions between the essential response regulator RpaB
703 and cyanobacterial circadian clock output. Proc Natl Acad Sci U S A 112:2198–
704 2203.

705 57. Takai N, Nakajima M, Oyama T, Kito R, Sugita C, Sugita M, Kondo T, Iwasaki
706 H. 2006. A KaiC-associating SasA-RpaA two-component regulatory system as a
707 major circadian timing mediator in cyanobacteria. Proc Natl Acad Sci U S A

103:12109–12114.

58. Steglich C, Lindell D, Futschik M, Rector T, Steen R, Chisholm SW. 2010. Short RNA half-lives in the slow-growing marine cyanobacterium *Prochlorococcus*. Genome Biol 11.

59. Jacquet S, Partensky F, Marie D, Casotti R, Vaulot D. 2001. Cell cycle regulation by light in *Prochlorococcus* strains. Appl Environ Microbiol 67:782–790.

60. Shalapyonok A, Olson RJ, Shalapyonok LS. 1998. Ultradian growth in *Prochlorococcus* spp. Appl Environ Microbiol 64:1066–1069.

61. Palacio AS, Cabello AM, García FC, Labban A, Morán XAG, Garczarek L, Alonso-Sáez L, López-Urrutia Á. 2020. Changes in Population Age-Structure Obscure the Temperature-Size Rule in Marine Cyanobacteria. Front Microbiol 11.

62. Ting CS, Hambleton E, McKenna J. 2008. Photosynthetic Response to Environmental Stress in *Prochlorococcus*. Photosynth Energy from Sun 1585–1588.

63. Swain PS, Elowitz MB, Siggia ED. 2002. Intrinsic and extrinsic contributions to stochasticity in gene expression. PNAS 99:12795–12800.

64. Thattai M, Van Oudenaarden A. 2001. Intrinsic noise in gene regulatory networks. PNAS 98:8614–8619.

65. Axmann IM, Dühring U, Seeliger L, Arnold A, Vanselow JT, Kramer A, Wilde A. 2009. Biochemical evidence for a timing mechanism in *Prochlorococcus*. J Bacteriol 191:5342–5347.

66. Rippka R, Coursin T, Hess W, Lichtle C, Scanlan DJ, Palinska KA, Iteman I,

731 Partensky F, Houmard J, Herdman M. 2000. Prochlorococcus marinus Chisholm
732 et al. 1992 subsp. pastoris subsp. nov. strain PCC 9511, the first axenic
733 chlorophyll a2/b2-containing cyanobacterium (Oxyphotobacteria). Int J Syst Evol
734 Microbiol 50:1833–1847.

735 67. Calvo-Díaz A, Morán XAG. 2006. Seasonal dynamics of picoplankton in shelf
736 waters of the southern Bay of Biscay. Aquat Microb Ecol 42:159–174.

737 68. Andrews S. 2020. FastQC: A quality control tool for high throughput sequence
738 data. Available online at:
739 http://www.bioinformatics.babraham.ac.uk/projects/fastqc.

740 69. Bolger AM, Lohse M, Usadel B. 2014. Trimmomatic: A flexible trimmer for
741 Illumina sequence data. Bioinformatics 30:2114–2120.

742 70. Kopylova E, Noé L, Touzet H. 2012. SortMeRNA: Fast and accurate filtering of
743 ribosomal RNAs in metatranscriptomic data. Bioinformatics 28:3211–3217.

744 71. Langmead B, Salzberg SL. 2012. Fast gapped-read alignment with Bowtie 2. Nat
745 Methods 9:357–359.

746 72. Anders S, Pyl PT, Huber W. 2015. HTSeq-A Python framework to work with
747 high-throughput sequencing data. Bioinformatics 31:166–169.

748 73. Gifford SM, Satinsky BM, Moran MA. 2014. Quantitative Microbial
749 Metatranscriptomics. Environmental Microbiology: Methods and Protocols.

750 74. Kempe H, Schwabe A, Crémazy F, Verschure PJ, Bruggeman FJ. 2015. The
751 volumes and transcript counts of single cells reveal concentration homeostasis
752 and capture biological noise. Mol Biol Cell 26:797–804.

753 75. Zhurinsky J, Leonhard K, Watt S, Marguerat S, Bähler J, Nurse P. 2010. A

754 coordinated global control over cellular transcription. Curr Biol 20:2010–2015.

755 76. Love MI, Huber W, Anders S. 2014. Moderated estimation of fold change and
756 dispersion for RNA-seq data with DESeq2. Genome Biol 15:1–21.

757 77. Chen S, Zhou Y, Chen Y, Gu J. 2018. Fastp: An ultra-fast all-in-one FASTQ
758 preprocessor. Bioinformatics 34:i884–i890.

759 78. Deng Z-L, Münch PC, Mreches R, McHardy AC. 2022. Rapid and accurate
760 identification of ribosomal RNA sequences via deep learning. Nucleic Acids Res
761 50:e60–e60.

762 79. Klemetsen T, Raknes IA, Fu J, Agafonov A, Balasundaram S V., Tartari G,
763 Robertsen E, Willassen NP. 2018. The MAR databases: Development and
764 implementation of databases specific for marine metagenomics. Nucleic Acids
765 Res 46:D693–D699.

766 80. Pruitt KD, Tatusova T, Maglott DR. 2005. NCBI Reference Sequence (RefSeq):
767 A curated non-redundant sequence database of genomes, transcripts and proteins.
768 Nucleic Acids Res 33:501–504.

769 81. Li H, Durbin R. 2009. Fast and accurate short read alignment with Burrows-
770 Wheeler transform. Bioinformatics 25:1754–1760.

771 82. Putri GH, Anders S, Pyl PT, Pimanda JE, Zanini F. 2022. Analysing high-
772 throughput sequencing data in Python with HTSeq 2.0. Bioinformatics 38:2943–
773 2945.

774 83. Cock PJA, Antao T, Chang JT, Chapman BA, Cox CJ, Dalke A, Friedberg I,
775 Hamelryck T, Kauff F, Wilczynski B, De Hoon MJL. 2009. Biopython: Freely
776 available Python tools for computational molecular biology and bioinformatics.

Bioinformatics 25:1422–1423.

84. Kumar L, Futschik ME. 2007. Mfuzz: A software package for soft clustering of microarray data. Bioinformation 2:5–7.

85. Schwämmle V, Jensen ON. 2010. A simple and fast method to determine the parameters for fuzzy c-means cluster analysis. Bioinformatics 26:2841–2848.

86. Package T, Pasculescu AA, Methods EC, Gene U. 2022. Package ‘ ClusterJudge ’ 1–17.

Figure legends

Figure 1. Growth rates, cell size and number of mRNA transcripts per cell in samples of *Prochlorococcus marinus* MIT9301 collected after long-term thermal acclimation. Between 3 and 7 biological replicate samples are represented depending on the temperature treatment and error bars report the standard deviation between replicates. On the top of each plot, the minimum (T_{min}), optimum (T_{opt}) and maximum temperature (T_{max}) are indicated and, additionally, in the upper left plot, temperature treatments where RNA samples were collected are shown with arrows. (A) Growth rate and size of MIT9301 cells along the thermal niche. (B) Estimates of mRNA transcripts per cell along the thermal niche in samples collected at day-time (left panel) and night-time (right panel). Letters denote statistical significant differences (ANOVA test, Tukey post-hoc test, $p < 0.001$).

Figure 2. Clusters of *Prochlorococcus marinus* MIT9301 genes according to their pattern of day- and night-time expression along the thermal niche. Within each cluster, right- and left-side panels represent day- and night-time expression of the same genes, respectively. Dot colours indicate local density at each point of the scatterplot, with red circles indicating a high density of dots. Line colours within each softcluster indicate the membership value assigned by the "Fuzzy c-means soft" clustering of each gene, ranging from 1 (red, high score) to 0.5 (blue, low score). Genes with a membership value lower than 0.5 are not plotted, neither included in the total number of genes for each cluster (but they are included in Table S5). Below each cluster, the 20-top expressed genes are shown in rank order plots, and the expression levels (measured as [mRNA]) and day/night log-2-fold expression ratio) of a selection of representative genes are shown. Day-time values appear as blue lines and night-time values as black lines. Between 3 and 7 biological replicate samples are represented depending on the temperature treatment and error bars

report the standard deviation between replicates. Asterisks in the plots denote significant differences in transcript concentration along the thermal gradient in day-time (blue asterisks) or night time (black asterisks) according to Kruskal-Wallis test (* $p< 0.05$, ** $p < 0.01$, *** $p < 0.001$). In the log2fold ratios, values above 0 represent preferential expression during day-time (highlighted in blue), while values below 0 represent preferential expression during night-time.

Figure 3. Cellular expression levels (measured as [mRNA]) in *Prochlorococcus marinus* MIT9301 during day-time (blue lines) and night-time (black lines) along the thermal niche of (A) RNA polymerase components including sigma factors, (B) Histidine kinases and other regulatory proteins, (C) genes involved in the stress response, and (D) Nitrogen and Phosphate acquisition genes. Asterisks denote significant differences in transcript concentration along the thermal gradient in day-time (blue asterisks) or night time (black asterisks) according to Kruskal-Wallis test (* $p< 0.05$, ** $p < 0.01$, *** $p < 0.001$). The softcluster membership of each gene is shown only for those cases where the probability score was > 0.80.

Figure 4. Schematic diagram showing some of the main components of the photosynthetic and carbon metabolism pathways in *Prochlorococcus*. Colours of genes (or their corresponding protein complexes) follow the same code of their respective softclusters in Figure 2.

Figure 5. Expression patterns of a selection of *Prochlorococcus* photosynthetic genes of Photosystem II (*psbA, psbJ*) and Photosystem I (*psaA, psaB, psaF*) along the thermal gradient 17 to 30ºC in experimental acclimations (as analysed in *P. marinus* MIT9301 by transcriptomics, left pannel) and *in situ* environmental conditions (as analysed in MIT9301-like reads identified in metatranscriptomes of the *Tara* Oceans dataset, right panel). In both cases, reads were normalized using DESeq2 and log-transformed. Linear

regression lines are shown for all genes with significant Spearman correlation coefficients at a p-value < 0.05 (indicated in the plots).

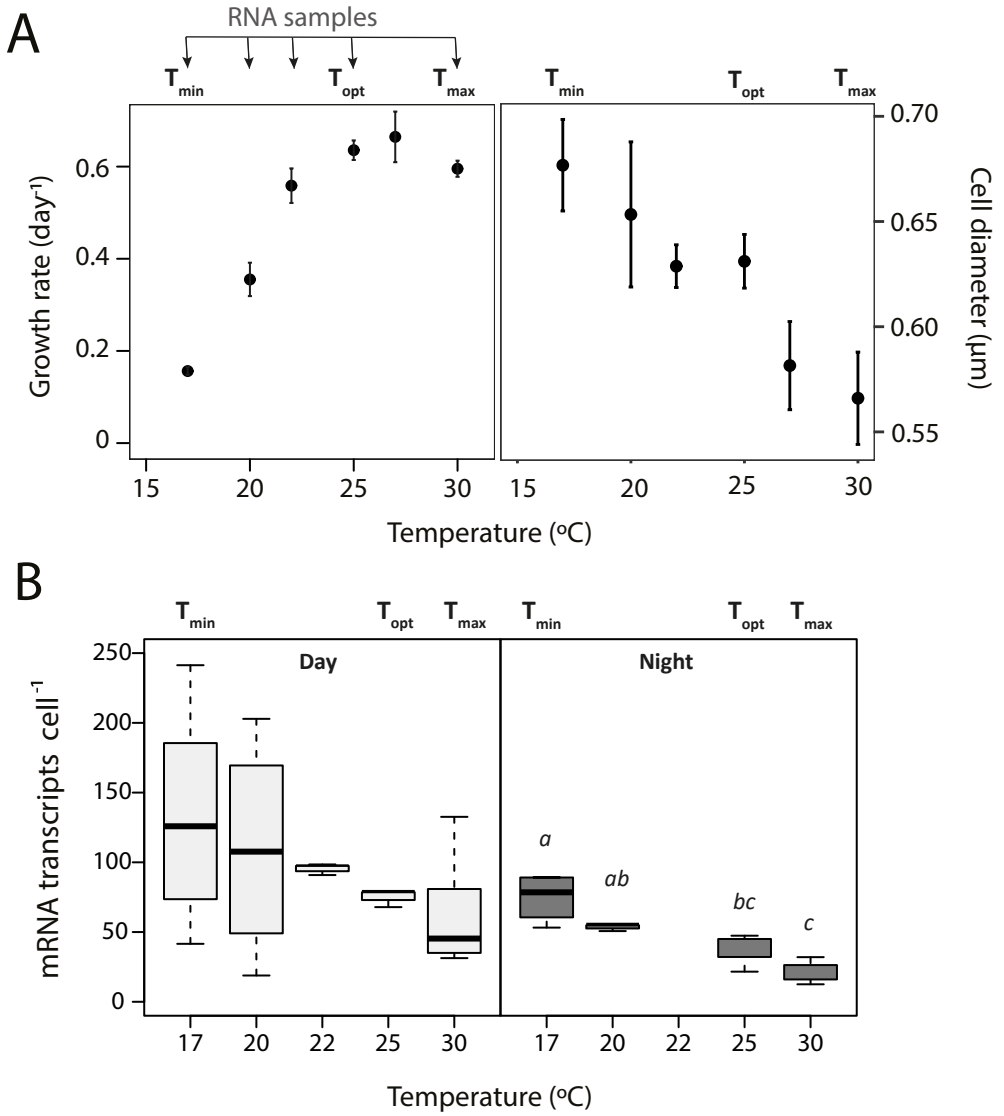
A
RNA samples
T min
T opt
T max
T min
T opt
T max
Growth rate (day-1)
0
0.2
0.4
0.6
Cell diameter (µm)
0.55
0.60
0.65
0.70
15
20
25
30
15
20
25
30
Temperature (ºC)
B
T min
T opt
T max
T min
T opt
T max
Day
Night
mRNA transcripts cell-1
0
50
100
150
200
250
a
ab
bc
c
17
20
22
25
30
17
20
22
25
30
Temperature (ºC)

Figure 1

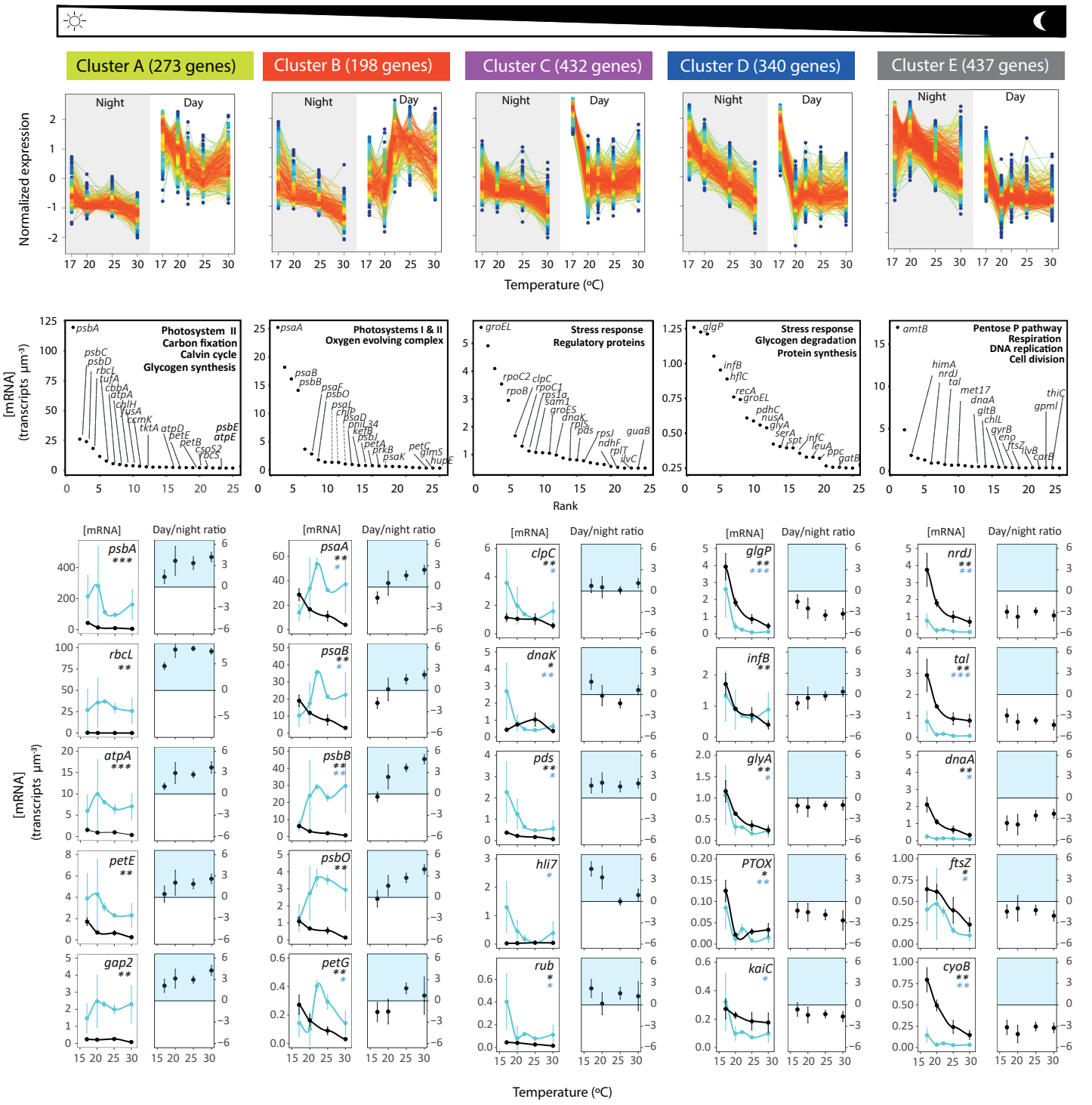
Cluster A (273 genes)
Cluster B (198 genes)
Cluster C (432 genes)
Cluster D (340 genes)
Cluster E (437 genes)
Night
Day
Normalized expression
Temperature (°C)
Photosystem II
Carbon fixation
Calvin cycle
Glycogen synthesis
Photosystems I & II
Oxygen evolving complex
Stress response
Regulatory proteins
Stress response
Glycogen degradation
Protein synthesis
Pentose P pathway
Respiration
DNA replication
Cell division
[mRNA] (transcripts µm⁻³)
Rank
[mRNA]
Day/night ratio
psbA
psaA
clpC
glgP
nrdJ
rbcL
psaB
dnaK
infB
tal
atpA
psbB
pds
glyA
dnaA
petE
psbO
hli7
PTOX
ftsZ
gap2
petG
rub
kaiC
cyoB
Day/Night Log2fold expression ratio

Figure 2

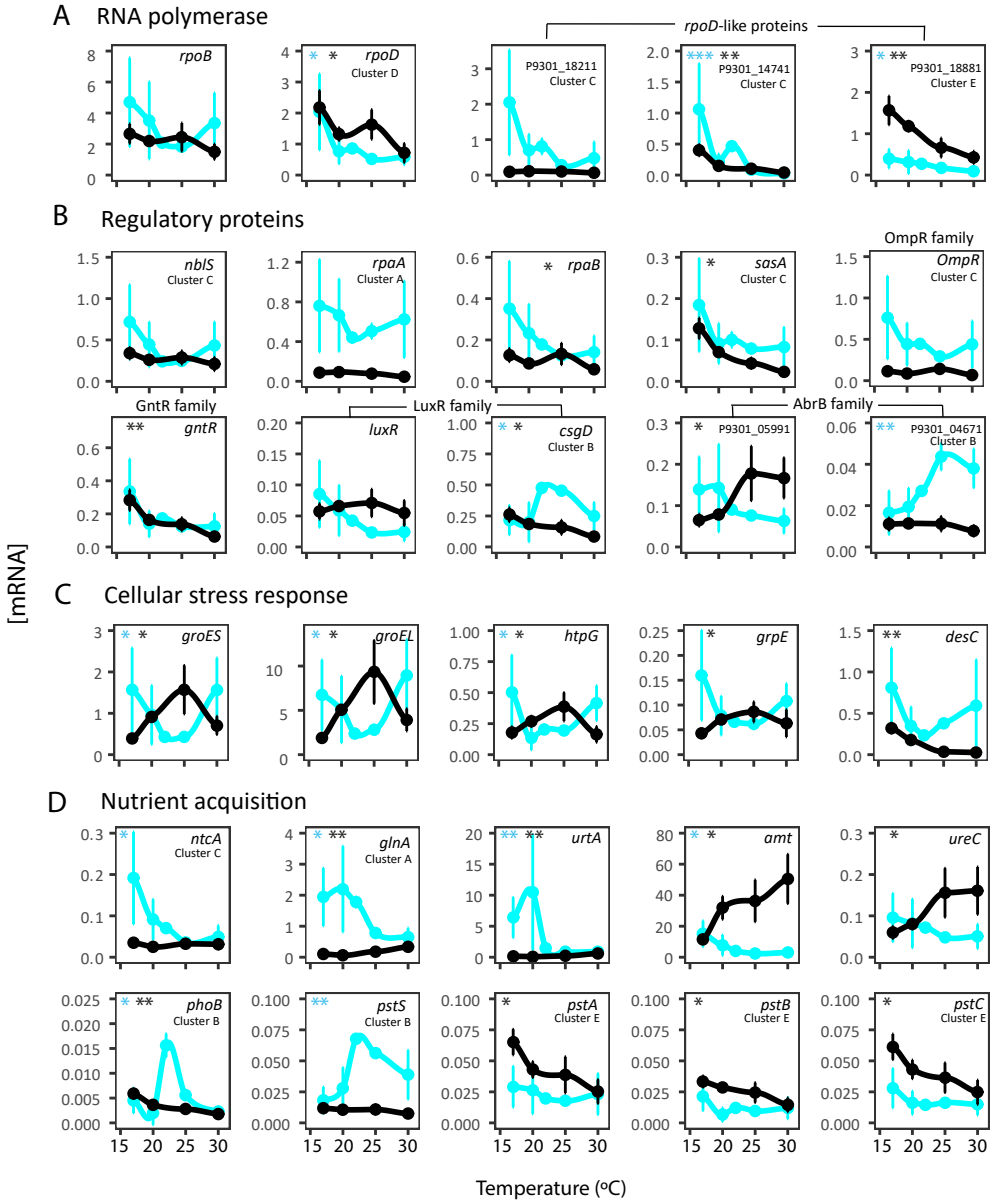
A RNA polymerase
rpoD-like proteins
rpoB
rpoD
Cluster D
P9301_18211
Cluster C
P9301_14741
Cluster C
P9301_18881
Cluster E
B Regulatory proteins
OmpR family
nblS
Cluster C
rpaA
Cluster A
rpaB
sasA
Cluster C
OmpR
Cluster C
GntR family
LuxR family
AbrB family
gntR
luxR
csgD
Cluster B
P9301_05991
P9301_04671
Cluster B
C Cellular stress response
groES
groEL
htpG
grpE
desC
D Nutrient acquisition
ntcA
Cluster C
glnA
Cluster A
urtA
amt
ureC
phoB
Cluster B
pstS
Cluster B
pstA
Cluster E
pstB
Cluster E
pstC
Cluster E
[mRNA]
Temperature (°C)

Figure 3

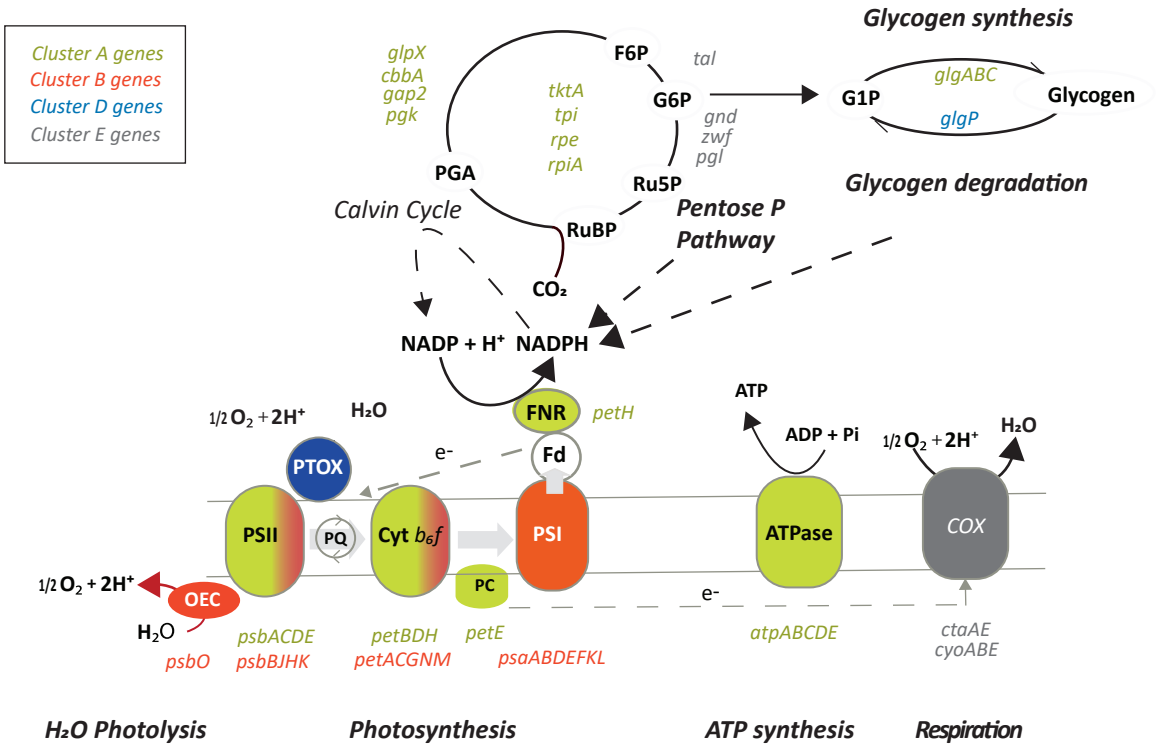
Cluster A genes
Cluster B genes
Cluster D genes
Cluster E genes
Glycogen synthesis
glpX
cbbA
gap2
pgk
F6P
tal
tktA
tpi
rpe
rpiA
G6P
gnd
zwf
pgl
G1P
glgABC
glgP
Glycogen
PGA
Ru5P
Glycogen degradation
Calvin Cycle
RuBP
Pentose P
Pathway
CO₂
NADP + H⁺
NADPH
ATP
ADP + Pi
1/2 O2 + 2H⁺
H₂O
FNR
petH
Fd
e⁻
PTOX
PSII
PQ
Cyt b6f
PSI
ATPase
COX
PC
OEC
H2O
psbO
psbACDE
psbBJHK
petBDH
petACGNM
petE
psaABDEFKL
atpABCDE
ctaAE
cyoABE
H₂O Photolysis
Photosynthesis
ATP synthesis
Respiration

Figure 4

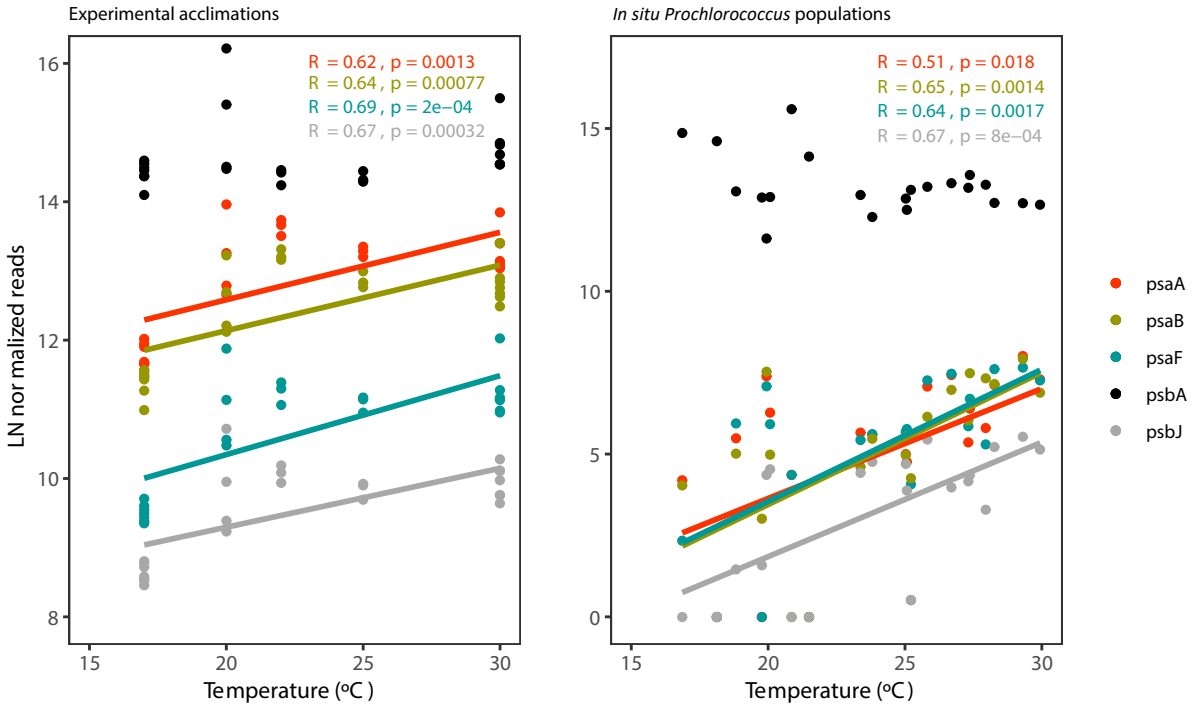
Experimental acclimations
R = 0.62 , p = 0.0013
R = 0.64 , p = 0.00077
R = 0.69 , p = 2e−04
R = 0.67 , p = 0.00032
LN nor malized reads
16
14
12
10
8
15
20
25
30
Temperature (°C)
In situ Prochlorococcus populations
R = 0.51 , p = 0.018
R = 0.65 , p = 0.0014
R = 0.64 , p = 0.0017
R = 0.67 , p = 8e−04
15
10
5
0
15
20
25
30
Temperature (°C)
psaA
psaB
psaF
psbA
psbJ

Figure 5